WATER RESOURCES RESEARCH, VOL. 37, NO. 2, PAGES 287–296, FEBRUARY 2001

Surface-zone flow along unsaturated rock fractures

Tetsu K. Tokunaga and Jiamin Wan

Earth Sciences Division, E. O. Lawrence Berkeley National Laboratory, Berkeley, California

Abstract. Although fractures in rock are well recognized as pathways for fast percolation of water, processes which permit fast flow along unsaturated fracture pathways remain to be identified and understood. Earlier aperture-based models of flow in partially saturated fractures permit fast flow only through a continuous network of locally saturated segments. Film flow was recently identified as a mechanism capable of sustaining fast flow along truly unsaturated fractures when the matric potential is very close to zero. Another mechanism for fast flow along unsaturated fractures is introduced in this study, "surface-zone flow," which can be important when the permeability of the rock along fractures (fracture skin) is significantly greater than that of the bulk rock matrix. In such systems the fracture surface zone provides low resistance pathways through which fast flow (relative to the bulk matrix rock) can occur, even when the fractures are at very low water saturation. Initial experimental tests of surface-zone fast flow were performed. Surface-zone fast imbibition of water was measured on a welded tuff and a rhyolite. However, because (1) imbibition rates are also strongly influenced by rock wettability, (2) these initially air-dry rocks exhibited finite contact angles upon exposure to water, and (3) we lack methods to reliably measure permeabilities of thin regions on rock surfaces, quantification of permeability contrasts was not possible in these initial tests.

1. Introduction

Our understanding of how water flows from the land surface downward through fractured rock is still quite limited, especially in unsaturated fractured rock common in arid and semiarid regions. Rapid migration of solutes through some portions of deep vadose (unsaturated) zones has recently been observed [*Nativ et al.*, 1995; *Fabryka-Martin et al.*, 1996]. Such findings show preferential water flow along a fraction of potentially conductive pathways and disequilibrium between fractures and the rock matrix. Some of the first conceptual models for flow and transport in unsaturated fractured rock require high fracture saturations in order to permit flow through fractures. Such models envision small regions of fractures as being either fully saturated or desaturated (Figure 1a), with the condition for local fracture saturation essentially based on aperture-capillarity considerations [*Wang and Narasimhan*, 1985; *Pruess and Tsang*, 1990]. In such conceptualizations, local segments within a fracture are either saturated (conductive) or dry (nonconductive), such that continuous saturated pathways within fractures are required to sustain fast flow. Until recently, transient pulses of locally highly saturated fracture flow during episodic, high-intensity rainfall events provided the only explanation for fast flow through fractured vadose zones [*Nitao and Buscheck*, 1991; *Wang et al.*, 1993]. However, evidence of rapid transport through unsaturated fractured rock often is not associated with evidence of either continuous or episodic saturated flow pathways [*Nicholl et al.*, 1994; *Glass et al.*, 1995]. Our search for mechanisms and conditions that permit fast flow and transport in truly unsaturated fractured rock is motivated in part by the need to resolve this paradox and in part by interest in examining alternative fast flow hypotheses.

Recently, film flow (Figure 1b) along water-filled surface-roughness features of unsaturated fractures was shown to permit fast, gravity-driven flow both as free surface flow [*Kapoor*, 1994] and when the matric potential is near zero [*Tokunaga and Wan*, 1997, 1998; *Or and Tuller*, 2000; *Tokunaga et al.*, 2000]. Water films along fracture surfaces can build up when the matric potential is high enough (close enough to zero) to sustain effectively saturated conditions in the immediately underlying matrix. The pore size distribution of the rock determines its satiation matric potential and hence the "near-zero" matric potential range over which water films can expand into local topographic depressions along fracture surfaces. As matric potentials increase toward zero, water films expand along fracture surfaces by first filling finer-scale roughness features and progressively filling coarser roughness features. "Film flow" can then occur along hydraulically continuous regions of thick "films" (filled topographic minima), with thin film regions (along topographic maxima) imposing most of the hydraulic resistance.

In the present study we propose another process which permits fast flow along unsaturated fractures and provide initial test results. This process, which we term "fracture surface-zone flow," can occur in fracture coatings, skins, or microcracked damage zones which have higher permeabilities than the underlying bulk rock matrix, when the local flux of water is high enough to sustain satiated water contents within fracture surface zones. Under such conditions, water is expected to flow preferentially within the fracture surface zone (Figure 1c). When the energy of pore waters in the fracture surface zone rises to its near-zero matric potential range, film flow becomes possible on the fracture surface. Thus surface-zone flow, local aperture saturation, and film flow can all contribute to flow along unsaturated fractures (Figure 1d). Under fully saturated fracture conditions the surface zone may only exhibit minor influence since flow is often dominated by continuous transmissive fracture aperture pathways. However, under conditions where fractures are unsaturated, and even when film flow

Paper number 2000WR900242.

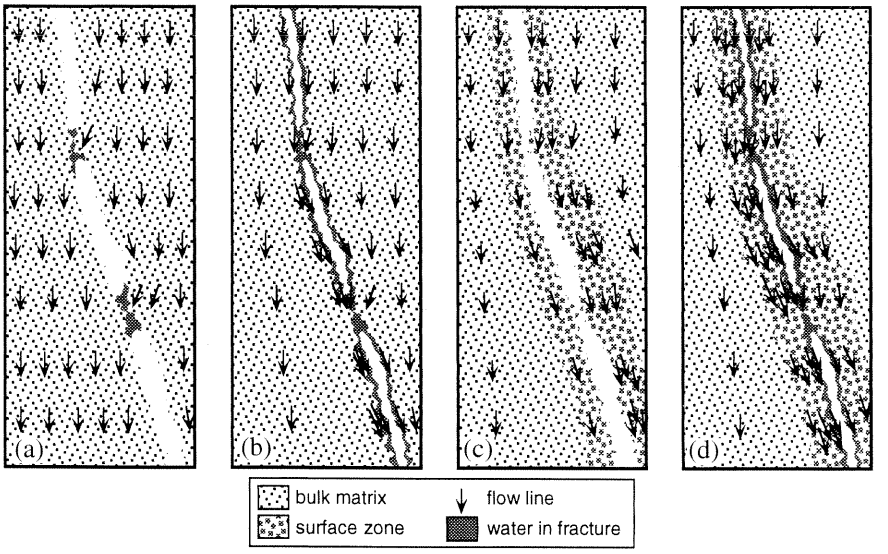

Figure 1. Contrasting conceptual models for (a) conventional aperture-based unsaturated flow, (b) film flow, and (c) surface-zone flow in unsaturated fractured rock. (d) When near-zero matric potentials develop for the fracture surface zone, flow can occur along the surface zone, in films, and in locally saturated apertures simultaneously. Note that high fracture saturations are generally needed in the aperture-based model before significant flow can occur along the fracture plane. When the fracture surface zone has a higher permeability than the underlying matrix rock, and/or when continuous transmissive films span unsaturated regions of fractures, fast flow of water can occur along partially saturated fractures relative to flow in the bulk matrix.

velocities are negligible, preferential flow within fracture surface zones might become important and diminish flow into the bulk rock matrix.

Two common features that can give rise to permeability enhancement within some fracture surface zones will be considered (recognizing that not all fracture surface zones are expected to have higher permeabilities than their underlying bulk matrix rock). The first type of feature is a mineral coating on a fracture surface having higher permeability than the underlying rock matrix. Studies of rock fracture coatings have emphasized mineralogy and geochemistry [e.g., *Carlos et al.*, 1993], as well as hydraulic properties [*Thoma et al.*, 1992; *Chekuri*, 1995]. However, previous hydrological studies on coatings addressed fracture-matrix interactions rather than flow along the fracture plane. Microcracks bounding fractures constitute a second type of feature that could enhance the surface-zone permeability. Although fracture microcracks have been studied in the context of rock mechanics [*Hoagland et al.*, 1973; *Kobayashi and Fourney*, 1978; *Swanson and Spetzler*, 1984; *Labuz et al.*, 1991], their possible importance in unsaturated fluid flow does not appear to have been investigated. Laboratory tests on these two types of fracture surface zones, fracture coatings and microcracks, will be presented in sections 3 and 4. It should be noted that processes leading to permeability enhancement within the fracture surface zone will be hydrologically most important in systems where the bulk matrix permeability is low. Because rocks of low matrix permeability are quite common, the possible significance of surface-zone fast flow along unsaturated fractures deserves examination.

Previous studies concerned with the hydrologic importance of the fracture surface zone (fracture skin) appear to have focused solely on matrix imbibition of water from fractures [*Thoma et al.*, 1992; *Chekuri*, 1995]. Such studies have addressed the importance of permeability contrasts in controlling rates of water flow from fractures into rock. It may be equally important to consider the influences of permeability contrasts on flow along the fracture plane, and this aspect of the fracture surface zone appears not to have been addressed in earlier studies. Upon including this second perspective on hydraulic effects of the fracture surface zone, it is interesting to note that contrasts in permeability between the surface zone and underlying matrix promote flow along the fracture plane, regardless of which region is higher in permeability. When the surface zone is very low in permeability relative to the matrix, flow is confined within the fracture aperture. When the surface zone has a much higher permeability than the underlying matrix, faster flow can occur along the unsaturated fracture plane, within this fracture skin. This second scenario is the focus of the present study. In common with these previous studies we utilized water imbibition experiments because they are potentially sensitive to permeability differences between the surface zone and bulk rock matrix.

2. Sorptivities and Permeabilities of Porous Media

Since this study relies on water-imbibition (sorptivity) measurements for identifying surface-zone flow, it is useful to review some basic aspects of this type of experiment. Although the sorptivity (S) of a porous medium depends upon both its initial water content and the water content maintained at the inflow boundary [*Philip*, 1957a], we will limit our considerations to S obtained from one-dimensional water imbibition from a free surface into initially air-dry porous media with the opposite end of the specimen open to atmospheric pressure. This amounts to imposing a source boundary at satiated water content (some air entrapment is likely) and approximately zero matric potential (small variations in gravitational potential along the fracture due to its topography impart variations in

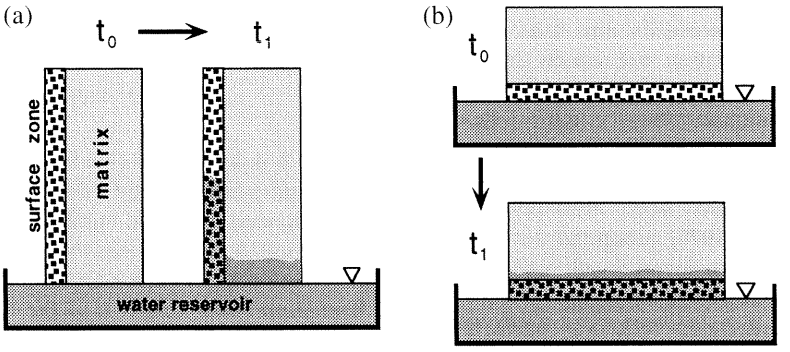

Figure 2. Orientation of fractured rock samples in the two types of imbibition experiments. (a) If the sample is oriented with the fracture surface vertical, perpendicular to the free water surface, imbibition can occur simultaneously through the fracture surface zone and the bulk matrix. If surface-zone fast flow is important, it is qualitatively evident from a more rapid wetting front advance along the fracture surface relative to the bulk matrix. (b) When the sample is oriented with the fracture surface faced downward and parallel to the free water surface, imbibition occurs first through the fracture surface zone and then into the bulk matrix.

surface pressure potential). In homogeneous porous media the short-term volumetric water uptake rate per unit area follows diffusion-like behavior. The early model of *Green and Ampt* [1911] assumes a constant matric potential at the wetting front and a step-function moisture profile with constant water content behind the wetting front. When the wetting front distance is small relative to the magnitude of the assumed wetting front matric head, the hydraulic potential gradient within the transmission zone is dominated by the matric potential gradient. Essentially identical models for transient liquid flow into capillary tubes were developed by *Bell and Cameron* [1906] and by *Washburn* [1921]. In all of these approaches the assumed constant wetting front matric (capillary) potential is interpreted in terms of a capillary pressure change at the advancing air-water interface, and the initial hydraulic potential of the system is not explicitly considered. The hydraulic potential gradient is dissipated as infiltration proceeds in all of these models, such that the short-time (negligible gravity) cumulative imbibition of water is linear with respect to the square root of time. Thus the Green-Ampt cumulative infiltration (I) is

$$I = \sqrt{2\Delta\theta\Delta\psi Kt}, \tag{1a}$$

where t is time, K is the effective hydraulic conductivity, $\Delta\theta$ is the step change in volumetric water content ($\Delta\theta \leq$ porosity), and $\Delta\psi$ is the magnitude of the constant matric head difference between the source and wetting front. The effective wetted distance (L) is directly related to the cumulative infiltration through the assumed step change in volumetric water content ($L = I/\Delta\theta$), and thus

$$L = \sqrt{\frac{2\Delta\psi Kt}{\Delta\theta}}. \tag{1b}$$

In more modern analyses of water absorption and infiltration into porous media [*Philip*, 1957a, 1957b, 1969] the cumulative infiltration is related to the square root of time through the sorptivity (S) when gravity is negligible,

$$I = S\sqrt{t}. \tag{2}$$

Thus, in the Green-Ampt approximation, the wetting front distance, sorptivity, and time are related through

$$L = \frac{S}{\Delta\theta}\sqrt{t}. \tag{3}$$

Although the sorptivity of a porous medium generally depends on the initial and final volumetric water contents, we will only consider the case of imbibition from free water sources into initially air-dry media. It should be noted that inferring hydraulic conductivities and hydraulic diffusivities from such processes can be problematic when considering porous media with incomplete or unknown wettability. We consider this limitation later in the context of interpreting experimental results.

Two types of imbibition experiments were considered for the purpose of identifying surface-zone flow. The first type of experiment imposes inflow parallel to the fracture plane and simultaneous wetting into the fracture surface zone and bulk matrix (Figure 2a). Qualitative indications of whether or not surface-zone imbibition is fast relative to matrix flow can be obtained by observing relative rates of wetting front advance in these two regions. Complexity of the internal flow field arises from differences in hydraulic properties, leading to flow from one region into the other. This complication, combined with difficulties of measuring the component inflows into the two regions, appears to prevent quantification of surface-zone flow by simple analyses. Inverse modeling [e.g., *Šimůnek and van Genuchten*, 1996; *Finsterle and Faybishenko*, 1999] has the potential to permit quantitative interpretation of this flow geometry. The second type of imbibition experiment imposes flow normal to the fracture plane by placing the fracture surface in contact with a water reservoir and inducing flow into the fracture surface zone and then into the bulk rock matrix (Figure 2b). Although the imposed flow (across the surface zone) is orthogonal to the flow direction of interest (along the surface zone), this approach retains the simplicity of one-dimensionality. For purposes of quantifying flow along the surface zone this flow geometry requires that the hydraulic conductivity functions for both the surface zone and bulk matrix be essentially isotropic. Lacking reliable methods for directly measuring each component of the permeability tensor within thin fracture surface zones (discussed later), we assume isotropic permeabilities.

When a transient flow process occurs along the direction

normal to layered heterogeneities, as in infiltration through a crust overlying a soil or in imbibition into bulk rock via a fracture surface zone, the infiltration rate reflects the hydraulic properties of both layers. The initial stage of infiltration, while the wetting front is still within the crust or coating, is described adequately by the previous approaches. However, once the underlying porous medium is encountered, the contrasting hydraulic characteristics of the two layers must be taken into account. *Hillel and Gardner* [1970] presented an analysis of transient infiltration into a crust-covered soil, based upon the Green-Ampt model. A similar study on water imbibition into fracture coatings and underlying rock was performed by *Thoma et al.* [1992], based on the *Washburn* [1921] approach. Both of these analyses showed that during the later stages, when the wetting front is within the underlying porous medium, the infiltration rate could be predicted based upon S or the hydraulic diffusivity (D) of the second medium. Thus the slope of I versus $t^{1/2}$ at later stages yields S of the underlying porous medium. *Hillel and Gardner* [1970] noted that the values of S and D characteristic of wetting front advance into the second layer will, in general, depend upon the hydraulic resistance imposed by the first layer because this resistance influences the matric potential at the contact between the two regions.

Analyses which are solely based on the Green-Ampt or Washburn models do not account for time-dependent changes in hydraulic resistance in the contact region between the crust and bulk porous medium. Such changes arise from the increasing matric potential (becoming less negative) in the contact region resulting in temporally increasing unsaturated hydraulic conductivity, and the study by *Ahuja* [1974] showed that this can yield inaccurate Green-Ampt-based results for high values of crust resistance. In our study we are only concerned with the opposite case, where the surface zone offers minor resistance relative to the lower-permeability interior rock. In such case a plot of $I(\sqrt{t})$ exhibits a steep initial slope followed later by a more gradual slope. These two regions correspond to the sorptivities of the surface zone and interior rock, respectively.

When considering possible surface-zone flow along unsaturated fractures, it is of greater interest to quantify contrasts in permeabilities of surface and bulk regions of rock, rather than their sorptivities for initially dry conditions. In many low-permeability rocks it can be expected that they often exist at relatively high water saturations in deep vadose environments. For example, water saturations in excess of 90% are common in measurements on core samples from the vadose zone at Yucca Mountain, Nevada [*Flint*, 1998]. High values of initial water saturation greatly reduce imbibition rates, as first quantitatively addressed by *Philip* [1957b]. In that study the sorptivity was shown to decrease approximately linearly with increased water saturation, with greater decreases at high saturation. Thus laboratory imbibition rates determined on initially dry samples greatly exceed rates relevant under field conditions.

Our consideration of sorptivity measurements in layered media is primarily motivated by the need to quantify surface-zone permeabilities. Thus, if sorptivity measurements on initially dry porous media could be used to estimate permeabilities, then imbibition experiments conducted on both the fracture surface zone and bulk rock could be useful in evaluating contrasts in flow between these two regions. *Kao and Hunt* [1996] showed that the wetting front distance depends on the one-fourth power of the permeability (k) for many porous media:

$$L = B\sqrt{\frac{\sigma}{\mu}}\,k^{1/4}\sqrt{t}, \tag{4}$$

where B is a constant ($\approx$0.5), σ is the liquid-gas surface tension, and μ is the liquid's dynamic viscosity. The above result was obtained for liquid imbibition into straight capillary tubes as the starting point [*Washburn*, 1921], assuming perfect wetting (zero contact angle). Combining (3) and (4) shows that the Kao-Hunt result relates k to the fourth power of S,

$$k \approx \left(\frac{\mu}{\sigma}\right)^2\left(\frac{S}{B\Delta\theta}\right)^4. \tag{5a}$$

For water imbibition displacing air in a strongly water wetting porous medium, at 20°C, (5a) gives

$$k[\mathrm{m}^2] \approx (3\times 10^{-3}\ \mathrm{s}^2\ \mathrm{m}^{-2})\left(\frac{S}{\Delta\theta}\right)^4, \tag{5b}$$

when $B = 0.5$ and when S has units of m s$^{-1/2}$. Thus relatively small differences in S reflect large differences in k. For example, even if the surface-zone sorptivity is only 3.2 times that of the underlying bulk matrix, the surface-zone permeability is approximately 100 times higher than that of the bulk rock (assuming both regions are highly wettable). On the basis of B values identified by *Kao and Hunt* [1996] being largely in the range of 0.3 to 0.7, the relative uncertainty in B is estimated to be about 0.4 (i.e., $B = 0.5 \pm 0.2$). Since k is correlated to B^{-4} and B is the dominant uncertainty, the relative uncertainty in k calculated using (5b) is about 0.8 when other uncertainties are negligible [*Taylor*, 1982]. Thus estimates of k ($\pm$80%) might be obtained through imbibition experiments and (5a) and (5b). While this level of uncertainty is large, (5b) remains sensitive to large permeability differences in highly wettable media. *Kao and Hunt* [1996] showed that (4) could be satisfactorily applied to imbibition data which spanned over 3 orders of magnitude in k (1.8×10^{-14} to 6.8×10^{-11} m^2).

It is worth noting here that there are at least two other approaches that also lead to the above result of permeabilities correlating to the fourth power of sorptivities. The first combines the Green-Ampt analysis with a correlation between the wetting front matric potential and the hydraulic conductivity. On the basis of capillary scaling, $\Delta\psi$ is proportional to $K^{-1/2}$ [*Miller and Miller*, 1956], such that (1a) leads directly to a sorptivity dependent on the one-fourth power of permeability for Miller-Miller similar media. Alternatively, the relation between the saturated hydraulic conductivity (K_{sat}), α parameter [*van Genuchten*, 1980], and sorptivity obtained by *Zimmerman and Bodvarsson* [1991] and by *Winterle and Stothoff* [1998],

$$S^2 \propto K_{\mathrm{sat}}/\alpha, \tag{6}$$

can be combined with the capillary scaling proportionality relation between α and K_{sat} proposed by *Wang and Narasimhan* [1992],

$$\alpha \propto \sqrt{K_{\mathrm{sat}}}, \tag{7}$$

to again relate sorptivity to the one-fourth power of permeability.

Although sorptivity-permeability correlations probably can be applied successfully in many systems, the above relations have limitations, and faster imbibition rates do not universally

reflect higher permeabilities. The uncertainty in sorptivity-estimated matrix permeability is potentially very large if (5b) is applied beyond the range of conditions encompassed by *Kao and Hunt* [1996], because of geometry, scale, and wettability influences. The more closed pore structure of the consolidated rocks we investigated are not expected to be geometrically similar to unconsolidated granular porous media for which (5b) applies. Furthermore, the lower permeabilities of the rocks used in this study indicate that their characteristic pore sizes are smaller than those of the media included in the work of *Kao and Hunt* [1996]. *Miller and Miller* [1956] anticipated breakdown of hydraulic scaling for geometrically similar media in the limit of very fine pores. The possibility that a scale dependence for the B factor would need to be incorporated into (5a) and (5b) was investigated in a part of this study described in sections 3 and 4. Finally, (5b) is not expected to apply for imbibition into porous media which are not strongly water wetting. Inspection of (4) and (5a) might suggest that wettability could be accounted for through a cos ϕ factor included with the surface tension (σ), where ϕ denotes the contact angle. However, the unique determination of contact angles on rough surfaces of porous media can be problematic [*Morrow*, 1975; *Drelich et al.*, 1996]. Even with knowledge of intrinsic wettability, contact angle scaling in porous media remains problematic because of nonunique relations between apparent contact angles and capillary pressure (interfacial curvature) at pore walls that diverge or converge [*Philip*, 1971]. For all of these reasons it can be difficult to quantitatively correlate imbibition rates to permeabilities in low-permeability rocks that are not strongly water wetting.

Despite the aforementioned limitations the simplicity of imbibition experiments makes (5b) an attractive potential estimator of permeability. As indicated previously, by conducting imbibition experiments in which water flows through the fractured rock surface, first through the surface zone and finally into the bulk matrix, values of S characteristic of both regions are obtained. Permeabilities of these two regions can then be estimated from their sorptivities through (5b), subject to the limitations discussed previously. This approach is especially useful for investigating thin surface zones with relatively high permeabilities since alternative methodologies can be problematic.

Before describing our sorptivity-based experiments, problems associated with alternative techniques for quantifying surface-zone flow will be briefly noted. Direct isolation of surface-zone samples by cutting is attractive since it could permit hydraulic measurements independent of the bulk rock. However, cutting of thin surface-zone samples is likely to compromise measurements through inducing cracking or microfracturing, thereby imparting artificially highly enhanced permeabilities. Alternatives that involve sealing at the fracture surface and measuring permeabilities of the surface zone and bulk matrix in parallel are problematic because of imperfect sealing along rough natural fracture surfaces. For example, the use of elastic sleeves and application of lateral confining pressures is effective in sealing smooth-wall cores but is of questionable value for rough, irregular surfaces. The other general approach toward sealing, using glues or resins, suffers from the problem of filling into near-surface, high-permeability pores and microcracks. The use of gas probe permeameters [*Goggin et al.*, 1988; *Tidwell and Wilson*, 1997] might be useful in measurements on relatively thick fracture surface zones (greater than $\approx$ 10 mm), but to our knowledge, measurement dimensions compatible with surface zones in our study (2 to 7 mm) have not been reported with this method.

Table 1. Bulk Rock Properties

	Welded Tuff	Rhyolite
Bulk density, Mg m^{-3}	2.24 ± 0.02	2.10 ± 0.04
Effective porosity	0.098 ± 0.005	0.108 ± 0.003
Measured matrix permeability, m^2		
Average	7E−17[a]	1.2E−15
Range	3.3E−17 to 9E−17	7E−16 to 2E−15
Estimated matrix permeability,[b] m^2	1.5E−20 (±1.2E−20)	9.7E−17 (±7.8E−17)

[a]Read 7E−17 as 7×10^{-17}.
[b]See equation (5).

3. Materials and Methods

Experimental tests of surface-zone fast flow were conducted on a sample of welded tuff and a rhyolite. The Topopah Spring welded tuff (Yucca Mountain) was bounded by a natural fracture surface with a coating consisting primarily of fine quartz and tridymite (determined by x-ray diffraction). The sample was cut into a block, 70 mm by 56 mm by 24 mm, with the fracture surface along one of the 70 mm by 56 mm sides. The rhyolite sample (Owens River Gorge, Mono County, California) included a cooling joint fracture surface. The rhyolite did not exhibit obvious mineralogical contrasts between the surface zone and bulk rock, but it did contain shallow microcracks on the cooling joint surface and in its matrix. The rhyolite sample was cut into a 71 mm by 43 mm by 31 mm block, with the cooling joint on one of the 71 mm by 43 mm sides. Bulk properties of these rock are listed in Table 1. Effective porosities are equated here with volumetric water contents of vacuum-saturated samples. Matrix permeabilities listed in Table 1 were measured using two independent transient methods on both rock types. These were the falling-head method using water [*Klute and Dirksen*, 1986] and pressure decay method using air [*Jones*, 1972]. Matrix permeabilities calculated from sorptivity measurements described later are also listed in Table 1 for comparison. Rock samples were sealed with epoxy into acrylic plastic permeameters for the permeability measurements after all sorptivity tests were completed. For specimens that included a fracture surface zone, flow was normal to the fracture surface. Permeability measurements using water were conducted following vacuum saturation of samples. Permeability measurements using air were slip-corrected using procedures described by *Jones* [1972]. Ranges of values reflect the fact that 2 to 4 different specimens of each rock type were measured, each in duplicate.

Qualitative observations of surface-zone fast flow were obtained through experiments in which water entered the sample block simultaneously through both the surface zone and bulk rock matrix (Figure 2a). The bottom surface (containing both matrix and an edge of a fracture surface zone) of an initially air-dry block was placed in contact with a free water reservoir at time zero. The rock and reservoir were enclosed under an inverted glass beaker to minimize evaporative water loss. All experiments were conducted at room temperature (22° ± 2°C for all experiments, with less than ±0.5°C variation within any single experiment). The wetting front advance along the nat-

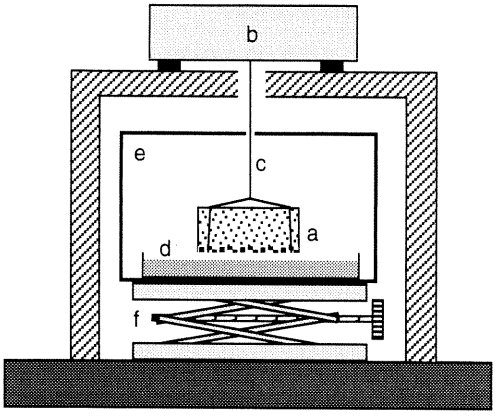

Figure 3. Apparatus for sorptivity measurements. The basic components are (a) the sample with horizontal area "a", electronic balance denoted by "b", sample hanging wire denoted by "c", water pan reservoir denoted by "d" with area "A", enclosure denoted by "e", and laboratory jack stand denoted by "f".

ural fracture and cut matrix surfaces was photographically recorded at various times during the imbibition process.

A more quantitative evaluation of surface-zone flow was obtained by conducting imbibition (sorptivity) tests with water entering through the surface zone and then into the bulk rock matrix (as in Figure 2b). A variety of similar methods have been used by other researchers [*Peters et al.*, 1987; *Chekuri*, 1995; *Humphrey et al.*, 1996; *Siebold et al.*, 1997]. The apparatus used for these imbibition experiments is shown in Figure 3. The initially air-dry rock sample is suspended from the bottom hook of an electronic balance (Sartorius LP1200-S) by a wire. The suspension wire is adjusted such that the lower surface of the rock is horizontal (within < 1 mm). The sample and water pan reservoir are contained within a chamber (desiccator box) to minimize evaporative water losses. The hole on the top surface of the chamber provides about 1 mm radial clearance between the chamber ceiling and the suspension wire. At time-zero the free water surface is placed in contact with the bottom surface of the rock by raising the chamber with the jack stand. The cumulative apparent imbibition mass indicated by the electronic balance is recorded as a function of time. The apparent imbibition mass is corrected for changes in buoyancy resulting from the small decline in the reservoir water level (Appendix A) and then is normalized to the horizontal surface area and expressed as cumulative imbibition. As shown in Appendix A, the buoyancy correction can be very important, depending on the relative areas of the free water surface and the fracture face. Measurements on a solid acrylic plastic block "blank" sample indicated that the background drift on the sorptivity apparatus was less than 0.02 g for the time intervals used in this work. Experiments were done for imbibition through the fracture surface into the bulk matrix and also for imbibition through "matrix only" samples. During experiments on flow through the fracture surface into the bulk rock the position of the visually observed wetting front was recorded at various times for later estimates of average volumetric water content. The "matrix only" samples included blocks of the same rock without a fracture surface and the blocks with fracture surfaces. In the latter case the fracture surface is oriented upward such that imbibition occurs directly into the matrix from the side opposite that of the fracture. Samples were oven-dried (105°C for 24 hours) after each test and rerun to test reproducibility.

As discussed in section 4, very large discrepancies between directly measured and sorptivity-estimated permeabilities were obtained for the rock specimens used in this study. The possible influences of wettability and scale were examined in an attempt to resolve these discrepancies. Wettabilities of initially air-dry rock were determined by measuring contact angles of water droplets placed on fracture surfaces and cut matrix surfaces, using a contact angle goniometer. The second possibility, that these rocks have characteristic pore scales smaller than the valid range for applying (5b), also needed testing. Recall that the lowest permeability included in the study by *Kao and Hunt* [1996] was 1.8×10^{-14} m^2. To test the possibility that B is scale-dependent, imbibition measurements were conducted on three highly wettable porous ceramics (Soilmoisture Equipment Corp., Santa Barbara, California) in order to determine the factor B (equation (5a)) based on measured sorptivities and the manufacturer's reported permeabilities. The 0.5, 3, and 15 bar ceramics used in our tests have permeabilities of 3.1×10^{-14}, 2.5×10^{-16}, and 2.6×10^{-18} m^2, respectively. Systematic deviations of calculated B values relative to the assumed value of 0.5 for the lower-permeability ceramics would indicate that the scaling limits were encountered in our study.

4. Results and Discussion

Both the welded tuff and rhyolite samples exhibited higher imbibition rates within their respective surface zones than within the bulk rock matrix. The higher sorptivity of the fracture surface zone of each rock was qualitatively revealed in the imbibition experiments conducted such that water enters directly into both the surface zone and bulk matrix (as in Figure 2a). For the welded tuff the wetting front within the surface zone advanced 4 to 7 times faster than in the bulk matrix (Figure 4a). For the rhyolite the wetting front advance was 2 to 3 times faster within the surface zone than in the bulk matrix (Figure 4b). These ratios of surface to bulk-region wetting front advance are next compared with sorptivity measurements on the same samples but with imbibition through the surface-zone and then into the bulk rock.

The cumulative imbibition of water into the welded tuff, via the fracture surface zone, exhibited initially higher S, followed by low S when the wetting front entered into the bulk matrix (Figure 5). Sorptivities measured in this manner were 2.9×10^{-5} m s$^{-1/2}$ and 4.8×10^{-6} m s$^{-1/2}$ for the surface zone and bulk matrix, respectively. The sorptivity measured directly on the matrix of the welded tuff was 4.3×10^{-6} m s$^{-1/2}$ (also shown in Figure 5), a value similar to that obtained in the second stage of imbibition through the fracture surface zone. Also, note that the ratios of S measured in the surface zone to that in the bulk rock are 6.0 and 6.7 (relative to the two measurements of matrix S), values in the range expected from the previously described imbibition experiments conducted with flow parallel to the fracture plane (ratios in the range of 4 to 7). The cumulative infiltration at the point of the change in slope for the experiments run with imbibition taking place through the fracture surface is associated with the wetting front being located at the interface between the surface zone and bulk matrix. For the measurements on the tuff the slope change occurs over the interval of $I = 0.43 \pm 0.10$ mm, rather than at a distinct value. Combining this information with

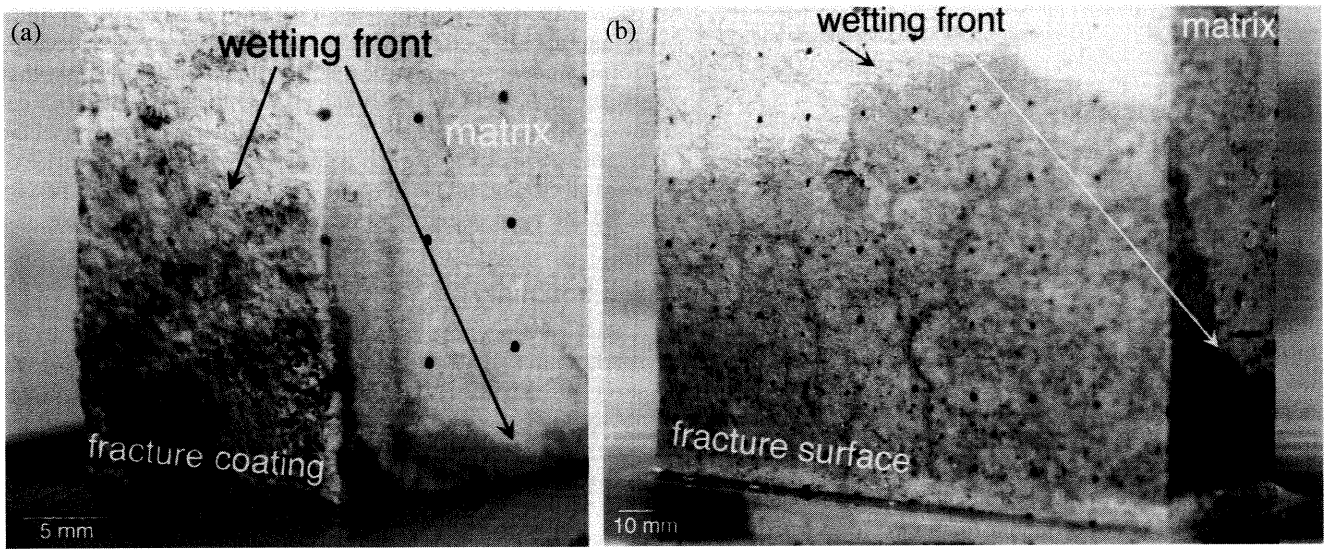

Figure 4. Upward imbibition of dyed water from a lower boundary maintained at a matric potential of −80 Pa. (a) Imbibition into initially dry Topopah Spring Tuff (welded), showing fast flow within the fracture coating (t = 25 min). (b) Imbibition into initially dry rhyolitic tuff, showing faster flow along the microfractured cooling joint surface (t = 26 min).

the visually observed wetting front position associated with this transition in sorptivities (L = 2.5 ± 0.4 mm), we obtain an estimate of the fracture surface-zone porosity equal to 0.17 ± 0.05. This effective porosity is higher than the bulk matrix effective porosity (0.098 ± 0.005).

Since permeabilities and hydraulic conductivities can be of greater interest than sorptivities, especially in long-term, large-scale processes, the aforementioned S values were used to estimate k values through (5b) and then were compared with directly measured bulk sample permeabilities. This comparison is important to perform because permeabilities calculated from imbibition measurements include critical assumptions about wettability, pore geometry, and scaling as mentioned in section 2. Combining the average of the two matrices S ($4.6 \times 10^{-6} \pm 0.3 \times 10^{-6}$ m $s^{-1/2}$) and the change in average volumetric water content in the wetted region ($\Delta\theta$ = 0.10 ± 0.01, based on measured cumulative imbibition divided by the wetted length as discussed below) in (5b) provides a sorptivity-estimated matrix permeability of 1.5×10^{-20} ($\pm 1.3 \times 10^{-20}$) m^2. The estimated uncertainty in k was calculated assuming that measurement uncertainties in B, $\Delta\theta$, and S can be treated as independent and even functions [*Taylor*, 1982; *Shoemaker et al.*, 1989] and that relative uncertainties in these terms are much larger than those for surface tension and viscosity. As noted in section 2, uncertainty associated with the B factor contributes the most to the uncertainty in the estimated permeability. Applying (5b) to the early time data for flow through the fracture surface of the welded tuff yields a surface-zone k of about $2.8 \times 10^{-18} \pm 2.3 \times 10^{-18}$ m^2, using the estimated $\Delta\theta = 0.17 \pm 0.02$ for this region. Thus, based on (5b), the thin surface zone of the tuff appears capable of conducting water about 170 times faster along the fracture plane than the underlying bulk rock matrix.

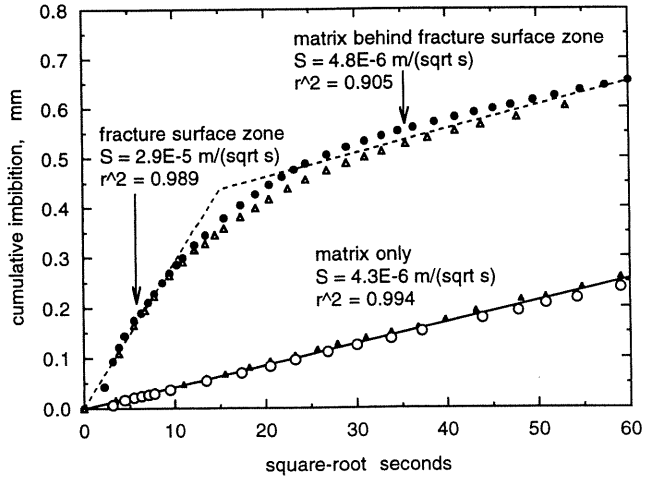

Figure 5. One-dimensional sorptivity experiments into a Topopah Spring Tuff. The upper curve is for imbibition through fracture surface coating into the matrix. The lower curve is for imbibition directly into the matrix. Different symbols show results from individual tests.

Independent direct measurements of the bulk rock yielded a much higher arithmetic mean matrix k of 7×10^{-17} m^2 (range of 3×10^{-17} to 9×10^{-17} m^2). These measurements (using both air and water as the permeating fluid) were made on the original specimen used in the sorptivity experiment and on other specimens cut from the original rock block. The very large (4700 fold) discrepancy between mean measured and estimated matrix permeabilities is far more than that attributable to uncertainties in B. The fact that the estimated permeability based on measured sorptivity is much lower than the directly measured permeabilities suggested that this rock is either not strongly wettable upon initial exposure to water or that (4) through (6) cannot be applied to low-permeability media because of scale dependence in B or both. The possibility that a scale dependence in B contributes to the observed inconsistency is addressed later. Contact angle measurements of water droplets placed on the initially air-dry tuff matrix and fracture surface yield values of 57° ± 8° and 23° ± 8°, respectively. These results indicate that wettability did, in fact, contribute to the discrepancy between direct and sorptivity-

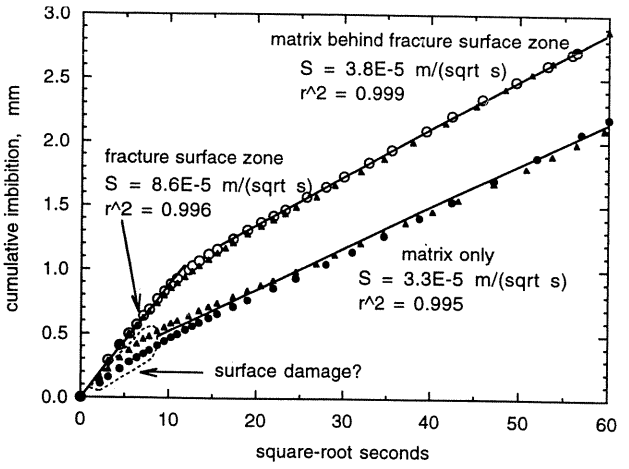

Figure 6. One-dimensional sorptivity experiments into an Owens Gorge rhyolite. The upper curve is for imbibition through fracture surface coating into the matrix. The lower curve is for imbibition directly into the matrix. Different symbols show results from individual tests.

estimated permeabilities, preventing inference of fast surface-zone flow from imbibition measurements.

Similar results, but with less sorptivity and permeability contrasts between the surface zone versus bulk rock, were obtained from experiments on the rhyolite (Figure 6). A higher initial sorptivity ($8.6 \times 10^{-5} \pm 0.7 \times 10^{-5}$ m $s^{-1/2}$) is observed relative to later stages of imbibition (3.8×10^{-5} m $s^{-1/2}$) for uptake through the fracture surface zone (upper curve in Figure 6). The measurements of imbibition directly into the matrix yielded a similar sorptivity (lower curve in Figure 6, with $S = 3.3 \times 10^{-5}$ m $s^{-1/2}$) as that obtained in the later stages of imbibition through the surface zone but also appear to reflect some loss of sample integrity during sawing of the original rock. This surficial damage is reflected in a short period of higher sorptivity as water initially wets the cut surface (Figure 6). The fracture surface zone S of 8.6×10^{-5} ($\pm 0.7 \times 10^{-5}$) m $s^{-1/2}$ is 2.4 times greater than the average S measured in the matrix ($3.6 \times 10^{-5} \pm 0.3 \times 10^{-5}$ m $s^{-1/2}$). The surface-zone volumetric water content change during imbibition ($\Delta\theta = 0.15 \pm 0.01$) was also significantly higher than that of the bulk matrix ($\Delta\theta = 0.087 \pm 0.008$). The estimated rhyolite matrix k based on its measured sorptivity, volumetric water content change ($\Delta\theta = 0.07 \pm 0.01$), and (5b) is 9.7×10^{-17} ($\pm 7.8 \times 10^{-17}$) m^2. From Eq. (5b), the estimated rhyolite surface-zone permeability of 3.6×10^{-16} ($\pm 2.9 \times 10^{-16}$) m^2 is about 4 times higher than this value. However, direct measurement of the saturated hydraulic conductivity of the rhyolite by falling head permeametry yielded k values from 7.0×10^{-16} to 2.0×10^{-15} m^2, again suggesting that partial water wettability is an important influence. Contact angle measurements on the dry rhyolite matrix and fracture surfaces yielded values of 40° ± 10° and 47° ± 8°, respectively, indicating that wettability is influencing imbibition. However, in this case the higher-sorptivity surface zone has a macroscopic wettability that is less than or equal to that of the bulk rock. Thus, although (5b) does not correctly predict the rhyolite matrix permeability, the available evidence still indicates that surface-zone fast flow does occur in this system.

Results of the imbibition experiments on the highly water-wettable ceramics showed no significant differences in the B parameter relative to the mean value of 0.5 (Figure 7), indicating that scale effects were not responsible for discrepancies between measured and calculated permeabilities. The fact that values of $B = 0.5$ were obtained for these fused matrix ceramics also suggests that this parameter is not strongly specific to pore geometry, since the data used by *Kao and Hunt* [1996] were all from granular porous media. Thus wettability appears to be the most general potential limitation of using (5b).

5. Summary

Surface-zone flow was identified as a process capable of resulting in faster flow along unsaturated fractures. When the surficial region of rock blocks is significantly higher in permeability than the overall rock matrix, flow within the surface zone can occur at proportionally higher velocities than in the bulk rock. Such surface-zone fast flow can occur even when the rock fractures are at very low water saturation. During recharge events the low sorptivity of partially saturated, very low permeability rock can sustain near-zero matric potentials along fracture surfaces associated with preferential flow paths. Alterations to the fracture surface zone of very low permeability rock are most likely to be permeability-enhancing, thereby permitting fast flow within the surface zone. Thus surface-zone flow can be important in contributing to flow through some unsaturated, fractured, low-permeability rock. In such environments, knowledge of bulk rock and fracture properties alone is insufficient for predicting hydrologic processes. Imbibition experiments demonstrated faster water uptake through the fracture surface zone than in the bulk matrix for a tuff and a rhyolite. However, quantitative determinations of surface-zone and matrix permeabilities were not obtained in these relatively low permeability and imperfectly wetting rock. Such quantification awaits development of techniques for directly measuring permeabilities within thin surface zones of rock fractures combined with appropriate analysis. The extension of gas probe permeametry to smaller dimensions might provide the necessary measurements. In general, flow experiments conducted over a range of short dimensions, combined with in-

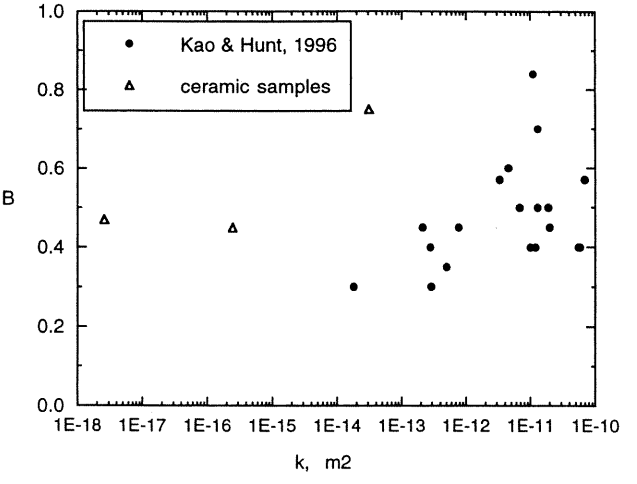

Figure 7. Correlation between permeabilities of the *Kao and Hunt* [1996] B parameter. The Kao and Hunt values are from their Table 1. The values for ceramics are based on the manufacturer's (Soilmoisture Equipment Corp., Santa Barbara, California) reported permeabilities and our measured sorptivities.

verse modeling, have the potential to identify fracture surface zones that do support fast flow.

Appendix A: Buoyancy Correction for Measuring the Water Uptake Mass

Readings obtained from the balance cannot generally be interpreted as being equivalent to the mass of water taken up by the porous medium because a finite submergence depth y requires a buoyancy correction. Furthermore, for typical applications y varies with time. Hence a necessary approximate correction for the time-dependent submergence depth is presented here. The possible influences of time-varying contact angle and surface tension are assumed to be negligible, based on the accurate calculations of mass change obtained with this approximate correction. The following analysis is expected to fail when the free water surface drops slightly below the lower surface of the rock such that changes in the air-water interfacial area become influential. The components of this analysis are shown in Figure A1. The oven-dry sample has an initial mass equal to its solid phase mass m_s. The sample height and uniform horizontal cross-sectional area are L and a, respectively. The reservoir has a total uniform cross-sectional area A and a free water surface area of A-a.

Time-dependent buoyancy corrections are potentially necessary from two sources contributing to variation in submergence depth. Relative to the stationary laboratory reference frame, the suspended sample descends during the course of water uptake, and the water level in the reservoir declines through flow into the porous medium. Measurements of the balance response to imposed displacements showed that the suspended sample descended at most 25 ± 5 μm. Such displacement contributed less than 10% to the buoyancy correction and was neglected. Thus the sample was considered stationary in these experiments, and the submerged depth was considered to decrease with time solely because of water transfer from the finite reservoir into the porous medium. At any instant in time the balance reading indicates the sum of the mass of solid and water within the sample and the buoyant mass of water displaced by the portion of the sample below the free surface. This application of Archimedes' principle gives

$$R = m_s + m_w - \rho_w a y, \tag{A1}$$

where m_s and m_w refer to the total sample mass and the total mass of water, respectively, imbibed into the porous medium at the time of obtaining the reading R and ρ_w is the density of water. The mass of the suspension wire need not be included because it amounts to a constant offset that is self-canceling when differences between readings at different times are calculated. The last term in (A1) is the submergence depth-dependent buoyancy correction for the total sample wet mass. Differentiating (A1) with respect to m_w gives

$$\frac{dR}{dm_w} = 1 - \rho_w a \frac{dy}{dm_w}. \tag{A2}$$

The change in imbibed water mass depends on the change in submergence depth through

$$dm_w = -\rho_w (A - a)\, dy. \tag{A3}$$

so that

$$\frac{dR}{dm_w} = \frac{A}{A - a}. \tag{A4}$$

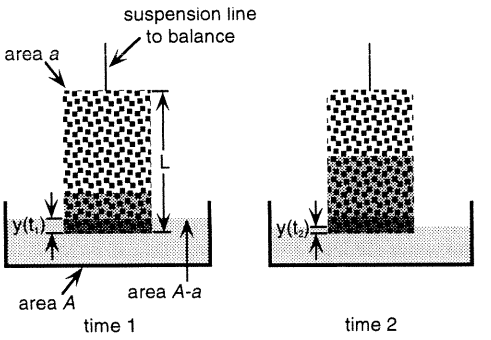

Figure A1. Buoyancy influence on imbibition mass measurements.

Integration of (A4) gives

$$m_w(t) = \left(1 - \frac{a}{A}\right)[R(t) - R(0)]. \tag{A5}$$

This result shows that changes in balance readings are larger than the associated water uptake in the porous medium and that neglecting uptake-dependent buoyancy effects will lead to erroneously high sorptivity values. Since the correction factor is $-a/A$, ignoring the buoyancy correction only provides reliable results when a/A is very small (i.e., for small samples in large area reservoirs). The above approximate expression was found to work satisfactorily, with balance readings corrected by the $-a/A$ factor agreeing within ±10% (average magnitude difference equals 5%) with direct measurements on sample mass increases. For the rock samples and water pan dimensions used in this study, neglecting this correction would have imparted systematic measurement errors ranging from +25% to +37%.

Acknowledgments. This work was carried out under U.S. Department of Energy (DOE) contract DE-AC03-76SF00098, with funding provided by the DOE, Basic Energy Sciences, Geosciences Research Program. We thank Stefan Finsterle and Larry Myer of LBNL for careful internal review and very helpful suggestions on the draft manuscript and James R. Hunt, Vincent C. Tidwell, and an anonymous reviewer for additional valuable comments on the final manuscript.

References

Ahuja, L. R., Applicability of the Green-Ampt approach to water infiltration through surface crust, *Soil Sci., 118*, 283–288, 1974.

Bell, J. M., and F. K. Cameron, The flow of liquids through capillary spaces, *J. Phys. Chem., 10*, 658–674, 1906.

Carlos, B., S. J. Chipera, D. L. Bish, and S. J. Craven, Fracture-lining manganese oxide minerals in silicic tuff, Yucca Mountain, Nevada, U.S.A., *Chem. Geol., 107*, 47–69, 1993.

Chekuri, V. S., The role of fracture coatings on water imbibition into unsaturated tuff at Yucca Mountain, M.S. thesis, Univ. of Nev., Reno, 1995.

Drelich, J., J. D. Miller, and R. J. Good, The effect of drop (bubble) size on advancing and receding contact angles for heterogeneous and rough solid surfaces as observed with sessile-drop and captive-bubble techniques, *J. Colloid Interface Sci., 179*, 37–50, 1996.

Fabryka-Martin, J. T., P. R. Dixon, S. Levy, B. Liu, H. J. Turin, and A. V. Wolfsberg, Summary report on chlorine-36 studies: Systematic sampling for chlorine-36 in the Exploratory Studies Facility, *Level 4 Milestone Rep. 3783AD*, Los Alamos Natl. Lab., Los Alamos, N. M., 1996.

Finsterle, S., and B. Faybishenko, Inverse modeling of a radial multistep outflow experiment for determining unsaturated hydraulic properties, *Adv. Water Resour., 22*(5), 431–444, 1999.

Flint, L. E., Characterization of hydrogeological units using Matrix properties, Yucca Mountain, Nevada, *U.S. Geological Survey: Water Resour. Invest. Rep. 97-4243*, 1998.

Glass, R. J., M. J. Nicholl, and V. C. Tidwell, Challenging models for flow in unsaturated, fractured rock through exploration of small scale processes, *Geophys. Res. Lett.*, *22*, 1457–1460, 1995.

Goggin, D. J., R. L. Thrasher, and L. W. Lake, A theoretical and experimental analysis of minipermeameter response including gas slippage and high velocity flow effects, *In Situ*, *12*, 79–116, 1988.

Green, W. H., and G. A. Ampt, Studies on soil physics, part I, The flow of air and water through soils, *J. Agric. Sci.*, *4*, 1–24, 1911.

Hillel, D., and W. R. Gardner, Transient infiltration into crust-topped profiles, *Soil Sci.*, *109*, 69–76, 1970.

Hoagland, R. G., G. T. Hahn, and A. R. Rosenfield, Influence of microstructure on fracture propagation in rock, *Rock Mech.*, *5*, 77–106, 1973.

Humphrey, M. D., J. D. Istok, L. E. Flint, and A. L. Flint, Improved method for measuring water imbibition rates on low-permeability porous media, *Soil Sci. Soc. Am. J.*, *60*, 28–34, 1996.

Jones, S. C., A rapid accurate unsteady-state Klinkenberg permeameter, *SPE J. Soc. Pet. Eng. J.*, *12*, 383–397, 1972.

Kao, C. S., and J. R. Hunt, Prediction of wetting front movement during one-dimensional infiltration into soils, *Water Resour. Res.*, *32*, 55–64, 1996.

Kapoor, V., Water film flow in a fracture in unsaturated porous medium, *Rep. CNWRA 94-009*, Cent. for Nucl. Waste Regul. Anal., San Antonio, Tex., May 1994.

Klute, A., and C. Dirksen, Hydraulic conductivity and diffusivity: Laboratory methods, in *Methods of Soil Analysis, Part 1, Physical and Mineralogical Methods, Soil Sci. Am. Book Ser.*, vol. 5, 2nd ed., edited by A. Klute, pp. 687–734, Am. Soc. Agron., Madison, Wis., 1986.

Kobayashi, T., and W. L. Fourney, Experimental characterization of the development of the micro-crack process zone at a crack tip in rock under load, paper presented at 19th U.S. Symposium on Rock Mechanics, Univ. of Nev., Reno, Stateline, 1978.

Labuz, J. F., C. N. Chen, and D. J. Berger, Microcrack-dependent fracture of damaged rock, *Int. J. Fract.*, *51*, 231–240, 1991.

Miller, E. E., and R. D. Miller, Physical theory for capillary flow phenomena, *J. Appl. Phys.*, *27*, 324–332, 1956.

Morrow, N. R., The effects of surface roughness on contact angle with special reference to petroleum recovery, *J. Can. Pet. Technol.*, *14*, 42–53, 1975.

Nativ, R., E. Adar, O. Dahan, and M. Geyh, Water recharge and solute transport through the vadose zone of fractured chalk under desert conditions, *Water Resour. Res.*, *31*, 253–261, 1995.

Nicholl, M. J., R. J. Glass, and S. W. Wheatcraft, Gravity-driven infiltration instability in initially dry nonhorizontal fractures, *Water Resour. Res.*, *30*, 2533–2546, 1994.

Nitao, J., and T. Buscheck, Infiltration of a liquid front in an unsaturated, fractured porous medium, *Water Resour. Res.*, *27*, 2099–2112, 1991.

Or, D., and M. Tuller, Flow in unsaturated fractured porous media: Hydraulic conductivity of rough surfaces, *Water Resour. Res.*, *36*, 1165–1177, 2000.

Peters, R. R., E. A. Klavetter, J. T. George, and J. H. Gauthier, Measuring and modeling water imbibition into tuff, in *Flow and Transport Through Unsaturated Fractured Rock, Geophys. Monogr. Ser.*, vol. 42, edited by D. D. Evans and T. J. Nicholson, pp. 99–106, AGU, Washington, D. C., 1987.

Philip, J. R., The theory of infiltration, 4, Sorptivity and algebraic infiltration equations, *Soil Sci.*, *84*, 257–264, 1957a.

Philip, J. R., The theory of infiltration, 5, The influence of the initial moisture content, *Soil Sci.*, *84*, 329–339, 1957b.

Philip, J. R., Theory of infiltration, *Adv. Hydrosci.*, *5*, 215–296, 1969.

Philip, J. R., Limitations on scaling by contact angle, *Soil Sci. Soc. Am. Proc.*, *35*, 507–509, 1971.

Pruess, K., and Y. W. Tsang, On two-phase relative permeability and capillary pressure of rough-walled rock fractures, *Water Resour. Res.*, *26*, 1915–1926, 1990.

Shoemaker, D. P., C. W. Garland, and J. W. Nibler, *Experiments in Physical Chemistry*, 5th ed., McGraw-Hill, New York, 1989.

Siebold, A., A. Walliser, M. Nardin, M. Oppliger, and J. Schultz, Capillary rise for thermodynamic characterization of solid particle surface, *J. Colloid Interface Sci.*, *186*, 60–70, 1997.

Šimůnek, J., and M. T. van Genuchten, Estimating unsaturated soil hydraulic properties from tension disc infiltrometer data by numerical inversion, *Water Resour. Res.*, *32*, 2683–2696, 1996.

Swanson, P. L., and H. Spetzler, Ultrasonic probing of the fracture process zone in rock using surface waves, paper presented at 25th U.S. Symposium on Rock Mechanics, Northwest. Univ., Evanston, Ill., 1984.

Taylor, J. R., *An Introduction to Error Analysis*, Univ. Sci., Mill Valley, Calif., 1982.

Thoma, S. G., D. P. Gallegos, and D. M. Smith, Impact of fracture coatings on fracture/matrix flow interactions in unsaturated, porous media, *Water Resour. Res.*, *28*, 1357–1367, 1992.

Tidwell, V. C., and J. L. Wilson, Laboratory method for investigating permeability upscaling, *Water Resour. Res.*, *33*, 1607–1616, 1997.

Tokunaga, T. K., and J. Wan, Water film flow along fracture surfaces of porous rock, *Water Resour. Res.*, *33*, 1287–1295, 1997.

Tokunaga, T. K., and J. Wan, Mechanisms for fast flow in unsaturated fractured rock, paper presented at 5th International Symposium on the Evaluation of Reservoir Wettability and its Effects on Oil Recovery, Statoil, Trondheim, Norway, June 22–24, 1998.

Tokunaga, T. K., J. Wan, and S. R. Sutton, Transient film flow on rough fracture surfaces, *Water Resour. Res.*, *36*, 1737–1746, 2000.

van Genuchten, M. T., A closed-form equation for predicting the hydraulic properties of unsaturated soils, *Soil Sci. Soc. Am. J.*, *44*, 892–898, 1980.

Wang, J. S. Y., and T. N. Narasimhan, Hydrologic mechanisms governing fluid flow in a partially saturated, fractured, porous medium, *Water Resour. Res.*, *21*, 1861–1874, 1985.

Wang, J. S. Y., and T. N. Narasimhan, Distributions and correlations of hydrologic parameters of rocks and soils, in *Indirect Methods for Estimating the Hydraulic Properties of Unsaturated Soils*, edited by M. T. van Genuchten, F. J. Leij, and L. J. Lund, pp. 169–176, U.S. Salinity Lab., Agric. Res. Serv., U.S. Dep. of Agric., Riverside, Calif., 1992.

Wang, J. S. Y., N. G. W. Cook, H. A. Wollenberg, C. L. Carnahan, I. Javandel, and C. F. Tsang, Geohydrological data and models of Rainier Mesa and their implications to Yucca Mountain, paper presented at High Level Radioactive Waste Management, 4th Annual International Conference, Am. Nucl. Soc., Inc., Las Vegas, Nev., 1993.

Washburn, E. W., The dynamics of capillary flow, *Phys. Rev.*, *17*, 273–283, 1921.

Winterle, J., and S. Stothoff, Evaluation of inconsistencies between laboratory-determined moisture retention characteristics and matrix sorptivity, in *Proceedings of FTAM: Field Testing and Associated Modeling of Potential High-Level Nuclear Waste Geologic Disposal Sites*, edited by G. S. Bodvarsson, *Rep. LBNL-42520*, pp. 31–33, Lawrence Berkeley Natl. Lab., Berkeley, Calif., Dec. 1998.

Zimmerman, R. W., and G. S. Bodvarsson, A simple approximate solution for horizontal infiltration in a Brooks-Corey medium, *Transp. Porous Media*, *6*, 195–205, 1991.

T. K. Tokunaga and J. Wan, Earth Sciences Division, E. O. Lawrence Berkeley National Laboratory, 1 Cyclotron Road, MS 90-1116, Berkeley, CA 94720. (tktokunaga@lbl.gov; jwan@lbl.gov)

(Received December 2, 1999; revised August 8, 2000;
accepted August 8, 2000.)